Histol Histopathol (2014) 29: 107-125
DOI: 10.14670/HH-29.107

http://www.hh.um.es

Histology and Histopathology
Cellular and Molecular Biology

Impaired hepatocyte maturation, abnormal expression of biliary transcription factors and liver fibrosis in *C/EBPα (Cebpa)*-knockout mice

Yusuke Akai, Takeshi Oitate, Toru Koike and Nobuyoshi Shiojiri
Department of Biology, Faculty of Science, Shizuoka University, Suruga-ku, Shizuoka City, Shizuoka, Japan

Summary. Inactivation of the C/EBPα gene (*Cebpa*) in the mouse not only causes impaired hepatocyte maturation, but also induces pseudoglandular structures in the liver parenchyma. The present study was undertaken to determine how the expression of other transcription factors controlling differentiation into hepatocytes and biliary epithelial cells is affected, and how the hepatic architecture, including the bile and vascular systems, is disordered in the fetal knockout liver. Histochemical analyses demonstrated that the expression of HNF1α and HNF4α was heterogeneous in the knockout liver, and that not all parenchymal cells (pseudoglandular) expressed these transcription factors, whereas parenchymal cells in the wild-type liver homogeneously expressed these transcription factors. SOX9, which was expressed only in biliary cells in the wild-type liver, was detectable in many pseudoglandular cells of the knockout liver. Although the pseudoglandular cells often coexpressed SOX9 and HNF1α/HNF4α, cells expressing SOX9 but not expressing HNF1α/HNF4α (biliary cells) were sometimes detectable in the parenchyma. Periportal biliary structures were abnormal in their segregation from the parenchyma and in their expression of the transcription factors and Ep-CAM, a biliary adhesion molecule. These results suggest that the inactivation of the *Cebpa* gene causes unstable expression of liver-enriched transcription factors or biliary transcription factors and elevated expression of Ep-CAM, which may lead to abnormal biliary morphogenesis in the knockout liver. The impaired maturation of the parenchyma caused elevated expression of PECAM-1, desmin and *Foxf1*, suggesting that the maturation of the parenchyma plays an important role in the normal histogenesis of nonparenchymal cells (stellate cells and sinusoidal endothelial cells).

Key words: C/EBPα, SOX9, Bile ducts, Hepatocytes, Differentiation

Offprint requests to: Nobuyoshi Shiojiri, Department of Biology, Faculty of Science, Shizuoka University, Oya 836, Sugura-ku, Shizuoka City, Shizuoka 422-8529, Japan. e-mail: sbnshio@ipc.shizuoka.ac.jp

Introduction

Intrahepatic bile ducts develop from hepatoblasts, which are liver progenitor cells in fetal stages of mammals, around portal veins under induction by the subjacent mesenchyme (Van Eyken et al., 1988a,b; Shiojiri et al., 1991; Shiojiri, 1997). After induction, periportal hepatoblasts are suppressed to express mature hepatocyte markers such as urea cycle enzymes, and give rise to biliary epithelial cells forming ductal plates or pearl-like structures and expressing osteopontin (secreted phosphoprotein 1; gene symbol, *Spp1*), bile-duct-type cytokeratins and Ep-CAM, which leads to the formation of intrahepatic bile ducts (Tanaka et al., 2009; Carpentier et al., 2011). TGFß/activin signaling or Jag1-Notch2 signaling is responsible for that induction (McCright et al., 2002; Tanimizu and Miyajima, 2004; Clotman et al., 2005; Hofmann et al., 2010; Si-Tayeb et al., 2010).

CCAAT/enhancer binding protein α (C/EBPα) is a member of the C/EBP family and belongs to the basic

leucine zipper class (bZIP) of transcription factors (Landschultz et al., 1989; Xanthopoulos et al., 1989; Nerlov, 2010; Tsukada et al., 2011). It engages in transcriptional regulation of genes for enzymes of gluconeogenesis and the urea cycle in the liver, and the inactivation of its gene causes the lack of some hepatic functions, including gluconeogenesis and detoxification of ammonia, and results in the development of pseudoglandular structures in the liver parenchyma (Wang et al., 1995; Flodby et al., 1996; Kimura et al., 1998; Tomizawa et al., 1998; Yamasaki et al., 2006). Although biliary epithelial cells differentiate around portal veins in the knockout liver, their bile duct morphogenesis is abnormal; periportal bile duct-like structures often connect with the pseudoglandular structures and are not segregated from the liver parenchyma (Yamasaki et al., 2006). However, it remains to be revealed in detail how hepatic functions and the expression of other liver-enriched transcription factors are impaired in hepatocyte populations, and how the hepatic architecture, including the bile and vascular systems, is disordered in the knockout liver. The action of C/EBPα may also be downstream of those of other liver-enriched transcription factors in an inter-transcription factor regulatory network in human hepatoma cells constituted by HNF1α, HNF3s (3α, ß, γ), HNF4α, Hhex, HNF6 and C/EBPs (Tomaru et al., 2009). The inactivation of genes coding for HNF6, HNF1ß and SOX9 causes impaired or delayed biliary development, indicating that these transcription factors play a pivotal role in this development (Clotman et al., 2002; Coffinier et al., 2002; Antoniou et al., 2009). The action of HNF1ß may be downstream from that of HNF6 (Clotman et al., 2002; Coffinier et al., 2002; Si-Tayeb et al., 2010). Comparison of the gene expression of these transcriptional factors in the *Cebpa*-knockout liver, including SOX9, HNF1ß, HNF6, HNF4α, HNF1α and the HNF3 family, with that in histological disorders may be useful to elucidate novel cell-cell interactions or tissue interactions, and the relationships among the transcription factors during development of the hepatic architecture.

In the present study, gene expression of various hepatocyte or biliary epithelial cell markers and transcription factors was examined in both wild-type and null livers, using RT-PCR, *in situ* hybridization and immunohistochemistry. Whereas liver-enriched transcription factors and biliary transcription factors were expressed in hepatocytes and biliary epithelial cells of the wild-type liver, respectively, their expression was conspicuously disordered in pseudoglandular cells of the knockout liver parenchyma. SOX9 and *Hnf1b* were strongly expressed in the knockout liver, and expression of HNF1α and HNF4α was suppressed in some pseudoglandular cells, indicating that the suppression of C/EBPα expression could directly induce biliary gene expression in hepatoblasts. The impaired maturation of the liver parenchyma also caused abnormal bile duct morphogenesis, activation of hepatic stellate cells, elevated deposition of collagens, and delayed maturation of sinusoidal endothelial cells, suggesting that the maturation of the liver parenchyma plays an important role in the normal histogenesis of these nonparenchymal cells.

Table 1. Primary antibodies used in immunohistochemistry.

Antibody	Immunogen	Source	Dilution
Rabbit anti-calf keratin antiserum	Bovine muzzle epidermal keratin subunits of 58, 56 and 52 k	Dako, Carpinteria, CA, USA	1:200
Rabbit anti-chicken desmin antiserum	Chicken gizzard desmin	Progen Biotechnik Gmbh, Heidelberg, Germany	1:100
Rabbit anti-human HNF4α antibodies (H-171)	Amino acids 295-465 of HNF4α of human origin	Santa Cruz Biotechnology, Santa Cruz, CA, USA	1:500
Rabbit anti-human HNF6 antibodies (H-100)	Amino acids 11-110 of HNF6 of human origin	Santa Cruz Biotechnology, Santa Cruz, CA, USA	1:200
Rabbit anti-mouse AFP antiserum	Mouse AFP	ICN Biochemicals, Aurora, OH, USA	1:100
Rabbit anti-mouse albumin antiserum	Mouse albumin	Cappel Laboratories, West Chester, PA, USA	1:100
Rabbit anti-mouse carbamoylphosphate synthase I (CPSI) antibody	C-terminus of CPSI of mouse origin	Nitou et al., 2002	1:500
Rabbit anti-rat type I collagen antiserum	Rat collagen type I	Chemicon International, Temecula, CA, USA	1:100
Rabbit anti-SOX9 antibodies	C-terminus of SOX9 of human origin	Millipore Corporation, Temecula, CA, USA	1:500
Rat anti-mouse Ep-CAM antibodies	TE-71 thymic epithelial cell line	Developmental Studies Hybridoma Bank	1:200
Rat monoclonal anti-mouse E-cadherin antibody (Clone: ECCD-1)	Mouse teratocarcinoma cell line F9	Takara Bio Inc., Otsu, Japan	1:100
Rat monoclonal anti-mouse PECAM-1 antibody (Clone: 390)		eBioscience, San Diego, CA, USA	1:100
Goat anti-human desmin antiserum (Y-20)	C-terminus of desmin of human origin	Santa Cruz Biotechnology, Santa Cruz, CA, USA	1:200
Goat anti-human HNF1α antibodies (C-19)	C-terminus of HNF1α of human origin	Santa Cruz Biotechnology, Santa Cruz, CA, USA	1:500
Goat anti-human HNF4α antibodies (C-19)	C-terminus of HNF1α of human origin	Santa Cruz Biotechnology, Santa Cruz, CA, USA	1:100
Goat anti-mouse osteopontin antibodies	NS0-derived, recombinant mouse osteopontin	R&D Systems, Minneapolis, MN, USA	1:100
Goat anti-mouse vimentin antiserum	Vimentin, isolated from a mouse fibroblast cell line	ICN Biochemicals, Aurora, OH, USA	1:200
Guinea pig anti-cytokeratin 8/18 antiserum	Bovine keratin K8/K18 filaments	Progen Biotechnik Gmbh, Heidelberg, Germany	1:100

Materials and methods

Materials

Knockout mice for the *Cebpa* gene were used (Flodby et al., 1996; Tomizawa et al., 1998; Yamasaki et al., 2006). The heterozygotes were mated during the night, and noon of the day the vaginal plug was found was considered 0.5 days of gestation. Fetuses at 13.5, 15.5 and 17.5 days of gestation, and newborns (1 day old) were used for immunohistochemistry and *in situ* hybridization. All animal experiments were carried out in compliance with the "Guide for Care and Use of Laboratory Animals" of Shizuoka University.

Histology and immunohistochemistry

For immunohistochemical examination of α-fetoprotein (AFP), albumin, carbamoylphosphate synthase I (CPSI), cytokeratins, osteopontin and transcription factors, or Sirius red and periodic acid-Schiff (PAS)-hematoxylin staining, tissues were fixed in a cold mixture of 95% ethanol and glacial acetic acid (99:1 v/v), and embedded in paraffin. Frozen sections (cold acetone-fixed for 10 min) were also used for immunohistochemistry of desmin, vimentin, PECAM-1, type I collagen and Ep-CAM. The antigens of HNF1α, HNF4α, HNF6 and SOX9 on paraffin sections were retrieved by TE (10 mM Tris, 1mM EDTA, 0.05% (w/v) Tween 20, pH 9.0) treatment at 95°C for 10 min after dewaxing.

Hydrated sections were incubated with the primary antibodies listed in Table 1 for 2 h at room temperature. Each primary antibody was monospecific in immunoblotting of the liver homogenate except for the anti-cytokeratin antisera. The anti-calf keratin antiserum reacted with 40-kDa (cytokeratin-19) and 54-kDa cytokeratin polypeptides in the detergent-resistant fraction of the liver homogenate (Shiojiri, 1994). The anti-cytokeratin 8/18 reacted with cytokeratin-8 and 18. The primary antibodies were diluted in 5% normal donkey serum (Jackson ImmunoResearch Lab., West Grove, PA, USA). After thorough washing with phosphate-buffered saline (PBS) containing 0.1% Tween; PBS/T), sections were incubated with a species-specific fluorochrome-labeled secondary antibody diluted in PBS/T (Table 2) for 1 h at room temperature, washed again, and mounted in buffered glycerol containing *p*-phenylenediamine (Johnson and de C Nogueira Araujo, 1981). In some immunofluorescence experiments, nuclei were stained with 4',6-diamidine-2'-phenylindole dihydrochloride (DAPI). Control incubations were carried out in 5% normal donkey serum in place of the primary antibodies. The specificities of the antibodies against transcription factors from Santa Cruz Technology were checked by preabsorption experiments with antigenic peptides.

When a peroxidase-labeled secondary antibody or streptoavidin-labeled peroxidase was used, endogenous peroxidase activity in sections was blocked by treatment with PBS containing 3% H_2O_2 for 10 min before incubation with the primary antibody. When biotinylated antibodies were used in immunohistochemistry, non-specific binding of avidin/biotin system reagents was blocked using an Avidin/Biotin Blocking Kit (Vector Laboratories, Burlingame, CA, USA) according to the manufacturer's instructions. In double immunostaining in the bright field using peroxidase-labeled or alkaline phosphatase-labeled antibodies, antibodies for visualization of the first antigen were removed by TE treatment (95°C, 10 min) before incubation with the primary antibody for the second antigen.

Hematoxylin-eosin (H-E) or PAS-H staining was carried out for demonstration of histology and glycogen, respectively. Collagen distribution was also visualized with picrosirius staining (Junqueira et al., 1979).

RT-PCR (reverse transcription-polymerase chain reaction)

Total RNA was extracted from developing livers using Isogen (Nippon Gene, Tokyo, Japan). Complementary DNA was synthesized from total RNA (0.5 μg) in 10 μl of reaction mixture containing 2.5 μM

Table 2. Secondary antibodies and labeled streptoavidin used in immunohistochemistry.

Antibody/Lebeled streptoavidin	Source	Dilution
Biotinylated donkey anti-goat IgG antibodies	Jackson ImmunoResearch Laboratories, West Grove, PA, USA	1:250
Biotinylated goat anti-rabbit IgG antibodies	Vector Laboratories, Burlingame, CA, USA	1:250
Cy3-labeled donkey anti-goat IgG antibodies	Jackson ImmunoResearch Laboratories, West Grove, PA, USA	1:500
Cy3-labeled donkey anti-rabbit IgG antibodies	Jackson ImmunoResearch Laboratories, West Grove, PA, USA	1:500
Fluorescein-labeled donkey anti-goat IgG antibodies	Jackson ImmunoResearch Laboratories, West Grove, PA, USA	1:200
Fluorescein-labeled donkey anti-rabbit IgG antibodies	Jackson ImmunoResearch Laboratories, West Grove, PA, USA	1:200
Fluorescein-labeled donkey anti-guiniea pig IgG antibodies	Jackson ImmunoResearch Laboratories, West Grove, PA, USA	1:200
Peroxidase-labeled donkey anti-rabbit IgG antibodies	Jackson ImmunoResearch Laboratories, West Grove, PA, USA	1:200
Streptoavidin-Alexa488	invitrogen, Carlsbad, CA, USA	1:500
Streptoavidin-Cy3	Jackson ImmunoResearch Laboratories, West Grove, PA, USA	1:900
Streptoavidin-labeled alkaline phosphatase	Jackson ImmunoResearch Laboratories, West Grove, PA, USA	1:1000
Streptoavidin-labeled peroxidase	Jackson ImmunoResearch Laboratories, West Grove, PA, USA	1:1000

Table 3. Primers used in RT-PCR analysis.

Gene name	Description	GeneBank	Sequence	PCR product length (bp)
Actb	ß-actin	NM_007393.3	F: 5'-GACGGCCAGGTCATCACTAT-3' R: 5'-ACATCTGCTGGAAGGTGGAC-3'	337
Afp	AFP	NM_007423.4	F: 5'-GGAGGCTATGCATCACCAGT-3' R: 5'-GTTCAGGCTTTTGCTTCACC-3'	165
Alb	Albumin	NM_009654.3	F: 5'-GTAGTGGATCCCTGGTGGAA-3' R: 5'-CTTGTGCTTCACCAGCTCAG-3'	179
Cdh1	Cadherin-1 (E-cadherin)	NM_009864.2	F: 5'-GCCAAGGCGCTGACAAACC-3' R: 5'-CCGGTGTCCCTATTGACAGT-3'	393
Cdh2	Cadherin-2 (N-cadherin)	NM_007664.4	F: 5'-CAACTTGCCAGAAAACTCCAG-3' R: 5'-TGATGATGTCCCCAGTCTCA-3'	500
Cebpb	C/EBPß	NM_009883.3	F: 5'-GCGGAACTTGTTCAAGCAG-3' R: 5'-ACACGTGTGTGTCGTAGTCC-3'	309
Cps1	Carbamoyl phosphate synthase I	NM_001080809.1	F: 5'-GCATTCATACCGCCTTCCTA-3' R: 5'-GCTCAGCAACACCAAGGAAT-3'	117
Des	Desmin	NM_010043.1	F: 5'-GTGAAGATGGCCTTGGATGT -3' R: 5'-GAAAAGTGGCTGGGTGTGAT -3'	319
Epcam	Epithelial cell adhesion molecule (Ep-CAM)	NM_008532.2	F: 5'-GGGTGAGATCCACAGAGAGC -3' R: 5'-GGGCAGCCTTAATCACAAAA-3'	400
Gapdh	Glyceraldehyde-3-phosphate dehydrogenase (GAPDH)	NM_008084.2	F: 5-'TGTTCCTACCCCCAATGTGT-3 R: 5-TGGCACACCATCATCTTGTT-3	396
G6pc	Glucose 6-phosphatase	NM_008061.3	F: 5'-CAAGGTAGATCCGGGACAGA-3' R: 5'-CCAGTCGACTCGCTATCTCC-3'	482
Foxa2	Forkhead box protein A2 (HNF3ß)	NM_010446.2	F: 5'-CCCGGGACTTAACTGTAACG-3' R: 5'-TCATGTTGCTCACGGAAGAG-3'	152
Foxa3	Forkhead box protein A3 (HNF3γ)	NM_008260.2	F: 5'-GCTACTACCCGGAGGCGGGC-3' R: 5'-CCGCCGGTACCCCTTTGCC-3'	293
Foxf1	Forkhead box protein F1	NM_010426.2	F: 5'-GAGTACCCGCACCACGAC -3' R: 5'-CACACACGGCTTGATGTCTT-3'	431
Hhex	Hematopoietically homoeobox protein Hhex	NM_008245.3	F: 5'-GAGGTTCTCCAACGACCAGA-3' R: 5'-TAGCCTTTATCCCCCTCGAT-3'	372
Hnf1a	HNF1α	NM_009327.3	F: 5'-CGTCCGCAAGCAGCGAGAGG-3' R: 5'-CTAGCCCCTGGGCCTGCGAT-3'	266
Hnf1b	HNF1ß	NM_009330.2	F: 5'-CGGCGACGACTATGACACTC-3' R: 5'-GCTTCTGCCTGAACGCCTCT-3'	692
Hnf4a	HNF4α	NM_008261.2	F: 5'-CTGGCAGATGATCGAACAGA-3' R: 5'-ATTGGTGCCCATGTGTTCTT-3'	160
Jag1	Jagged1	NM_013822.5	F: 5'-AGTAAACGGGATGGAAACAG-3' R: 5'-GCGGTGCCCTCAAACTCT-3'	583
Jag2	Jagged2	NM_010588.2	F: 5'-CTGGATGGAAGACTGCAACA-3' R: 5'-AGCCACAGCACACTGAACAC-3'	642
Onecut1(Hnf6)	One cut homeobox 1 (HNF6)	NM_008262.3	F: 5'-AAAGAGGTGGCGCAGCGTAT-3' R: 5'-GTTGGAGCCGCCCTCGTC-3'	471
Pecam1	Platelet endothelial cell adhesion molecule (PECAM-1)	NM_008816.2	F: 5'-TGCCTTGTTCATGTTGGGTA-3' R: 5'-ATTGCTGGCTTGAGGTCTGT-3'	417
Sox9	SRY-box containing gene 9 (SOX9)	NM_011448.4	F: 5'-CTGGCCAGATGGACCCACCA-3' R: 5'-TGCAGCCAGCAAGCAGGCAA-3'	767
Spp1	Secreted phosphoprotein 1 (Osteopontin)	NM_001204203.1	F: 5'-GCAGTCTTCTGCGGCAGGCA-3' R: 5'-ACCTCGGCCGTTGGGGACAT-3'	494
Tat	Tyrosine aminotransferase	NM_000353.2	F: 5'-GTCCGCATTGGACTTAAGGA-3' R: 5'-GCTTGTCTCGTGGTCAACAA-3'	426
Tdo2	Tryptophan 2, 3-dioxygenase	NM_019911.2	F: 5'-TTTCCAGGATTGGACCAAAA-3' R: 5'-GACACGCTCATGACCAAATG-3'	401

F, forward primer; R, reverse primer.

oligo dT primer, 0.25 mM dNTP, 2 U/μl RNase inhibitor, and 10 U/μl PrimeScript® II Reverse Transcriptase (Takara Bio Inc., Otsu, Japan), according to the manufacturer's instructions.

PCR reaction was conducted in 10 μl of the reaction mixture, using Ex-Taq DNA polymerase (Takara Bio Inc.; 0.025 U/μl). Primers listed in Table 3 were used at 0.5 μM. After various dilutions of template cDNA, we optimized the concentration for each primer. In these concentrations, amplification by PCR did not reach a plateau and could be used for semi-quantitative analysis. PCR cycles were as follows: initial denaturation at 94°C for 1.5 min, followed by 25-35 cycles at 94°C for 30 sec, at 60°C for 30 sec, at 72°C for 1 min, and final extension at 72°C for 10 min. PCR products were separated by 1% agarose gel electrophoresis.

In situ hybridization

cDNAs coding for partial sequences of mouse *Spp1, Hnf1b, Hnf6* (*Onecut1* - Mouse Genome Informatics), *Sox9,* and *Jag1* mRNAs were cloned by RT-PCR. The primers used were designed based on the sequences of mouse genes (DDBJ/EMBL/GenBank) (Table 4). Both sense and antisense digoxigenin-labeled riboprobes were synthesized from plasmids containing their cDNAs, and the rat cDNAs of AFP and albumin (gifts from Drs. T. Mitaka and S. Nishi, respectively) (Sargent et al., 1981) by using a DIG RNA labeling kit (Roche Diagnostics, Mannheim, Germany).

In situ hybridization on frozen sections was carried out according to Ishii et al. (1997) with some modifications, which included changing the hybridization temperature from 70 to 65°C. The proteinase K concentration was 2 μg/ml, and the length of the proteinase K treatment was modified according to the size of the tissue.

Results

Histogenesis of wild-type and knockout livers

Precursor structures of intrahepatic bile ducts, ductal plates or pearl-like structures, which had clear lumina and comparatively strong immunoreactivities to anti-calf cytokeratin antiserum, started to develop around portal veins at E13.5 in the wild-type liver (Fig. 1A). At E15.5, epithelial cells of the ductal plates, which were directly adjacent to portal mesenchyme, were cuboidal or squamous, and more strongly immunostained for cytokeratins than those on the parenchymal side ('asymmetrical' expression of cytokeratins) (Fig. 1C). At E17.5, intrahepatic bile ducts consisting of squamous epithelial cells, all of which expressed cytokeratins at almost the same level ('symmetrical' expression of cytokeratins), appeared in addition to many immature bile duct progenitors around portal veins (Fig. 1E). At E17.5-P0, hepatocytes lost the immunoreactivity to anti-cytokeratin antiserum (Fig. 1G). Although the histology of the E13.5 knockout liver was similar to that of the wild-type liver (Fig. 1B), strongly cytokeratin-positive pseudoglandular structures developed in the parenchyma at E15.5-17.5, including periportal, pericentral and pericapsular regions (Fig. 1D,F). This phenotype was in contrast to that of the wild-type liver, in which cytokeratin-positive bile structures were restricted to the portal area (Fig. 1C,E). Hematopoietic cells were still prominent in the E17.5 and P0 knockout livers, compared with wild-type livers at the same stages. At P0, intrahepatic bile ducts did not develop around portal veins in the knockout liver (Fig. 1H).

Expression of hepatocyte markers

RT-PCR analyses demonstrated that mRNA expression of several liver-specific enzymes, including CPSI (*Cps1*), glucose 6-phosphatase (*G6pc*), tyrosine aminotransferase (*Tat*) and tryptophan 2, 3-dioxygenase (*Tdo2*), was remarkably reduced in the knockout liver at E17.5, compared with the wild-type liver (Fig. 2B). By contrast, mRNA expression of AFP and albumin was not reduced in the E17.5 knockout liver (Fig. 2A).

PAS staining demonstrated that most hepatocytes poorly accumulated glycogen in the E17.5 knockout liver. CPSI protein expression was also severely impaired in pseudoglandular structures of the knockout liver (data, not shown). *In situ* hybridization analyses of *Afp* and *Alb* mRNAs demonstrated that their expression was not different between wild-type and knockout livers; hepatocytes and parenchymal pseudoglandular cells were positive but periportal bile duct progenitors were negative for both mRNAs (data, not shown). Asymmetrical expression of *Afp* and *Alb* was observed in the ductal plates of both wild-type and knockout livers. Immunohistochemical detection of AFP and albumin also showed a similar expression pattern to the data of the *in situ* hybridization analysis (data, not shown).

Expression of biliary markers

When gene expression of biliary markers *Spp1* and *Epcam* was examined using RT-PCR analysis, both markers were remarkably upregulated in the knockout liver (Figs. 3A, 4A). *Cadh1* (E-cadherin) expression was highly upregulated in the knockout liver (Fig. 4A). *In situ* hybridization analysis demonstrated that *Spp1* expression often exhibited a mosaic pattern of positive cells and negative cells in the knockout liver, including periportal bile duct progenitors, whereas that in the wild-type liver was limited to periportal biliary cells; there were no *Spp1*-positive cells in the liver parenchyma, including around central veins and under the hepatic capsule (Fig. 3B-E). Pseudoglandular cells under the hepatic capsule were prominently positive for *Spp1* expression in the knockout liver (Fig. 3C). Immunohistochemical analysis of *Spp1* protein (osteopontin) also showed that while wild-type livers

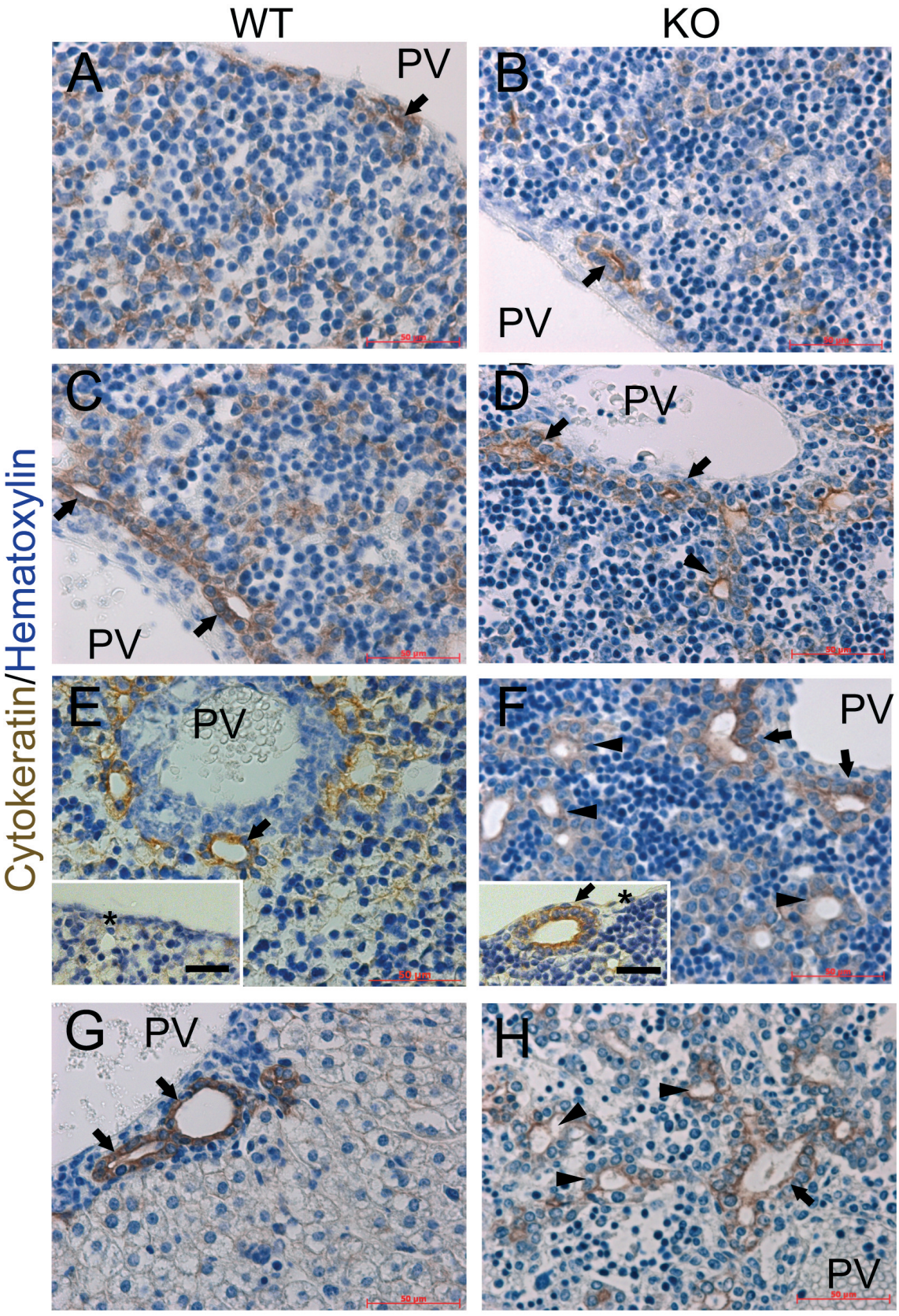

Fig. 1. Pseudoglandular structure development in the *Cebpa* knockout liver. **A, C, E, G.** Wild-type livers at E13.5, E15.5, E17.5 and P0, respectively. **B, D, F, H.** Knockout livers at E13.5, E15.5, E17.5 and P0, respectively. Liver sections were immunostained for cytokeratins using polyclonal anti-calf keratin antiserum. In both wild-type and knockout livers at E13.5, ductal plate structures (arrows), which show comparatively strong immunoreactivity to anti-keratin antiserum and have lumina, are detectable around portal veins (**A, B**). Whereas ductal plate structures (arrows) are confined to periportal area in wild-type livers, pseudoglandular structures (arrowheads) are developed in the liver parenchymal region of the knockouts (**C-F**). Although hepatocytes are detectable under the hepatic capsule of the wild-type liver (inset of **E**), strongly cytokeratin-positive pseudoglandular structures are developed in the knockout liver (arrow; inset of **F**). Asterisks indicate the hepatic capsule. Intrahepatic bile ducts (arrows) develop around a portal vein in P0 wild-type liver (**G**). In the knockout liver at P0, pseudoglandular structures (arrowheads) are still prominent (**H**).

Arrows in the knockout livers (**D, F, H**) indicate pseudoglandular structures around portal veins. More hematopoietic cells are observed in knockout livers at E17.5 and P0 **(F, H)**. PV, portal vein. Bars: A-H, 50 μm; insets of E and F, 25 μm.

expressed osteopontin only in the periportal biliary epithelial cells, the knockout livers had osteopontin expression in periportal biliary cells and pseudoglandular cells, the pattern of which was also mosaic, especially for the cytoplasmic staining (data, not shown). Expression of Ep-CAM and E-cadherin was also highly upregulated in the knockout liver, especially in the parenchymal region (Fig. 4B-E).

Expression of liver-enriched transcription factors and biliary transcription factors

Because several liver-specific or biliary marker genes were upregulated or downregulated in the knockout liver, gene expression of liver-enriched and biliary transcription factors was compared between wild-type and knockout livers. Gene expression of *Foxa2, Foxa3, Hnf1a,* and *Hnf4a* did not differ between the wild-type and knockout livers in RT-PCR analyses (Fig. 5A). However, *Cebpb* gene expression was downregulated in the knockout liver. Biliary transcription factors *Hnf1b, Hnf6* and *Sox9* were upregulated in the knockout liver (Fig. 5B).

Immunohistochemical analysis showed that all parenchymal cells expressed HNF1α and HNF4α in the wild-type liver, but periportal biliary cells never expressed them (Fig. 6A). Asymmetric expression of HNF1α and HNF4α was detectable in periportal bile duct structures. By contrast, in the knockout liver, most parenchymal pseudoglandular structures expressed HNF1α and HNF4α, though some negative cells were detectable (Fig. 6B). Expression of HNF1α and HNF4α had a mosaic-type pattern especially in the second layer of ductal plates. Double immunofluorescent analysis of HNF1α and HNF4α showed that both transcription factors were coexpressed in the nuclei of parenchymal cells in both the wild-type and knockout livers (data, not shown).

Whereas SOX9 protein expression was detectable only in biliary epithelial cells in the wild-type liver (Fig. 7A,C), it was observed not only in periportal biliary cells but also in liver parenchymal cells in the knockout liver (Fig. 7B,D). Pseudoglandular cells under the hepatic capsule and around central veins expressed SOX9 except for those around portal veins (Fig. 7B). Mosaic expression consisting of positive cells and negative cells was clearly detectable for SOX9 in these pseudoglandular cells (Fig. 7D). Sox9 mRNA expression showed a similar pattern of SOX9 protein expression (data, not shown). *In situ* hybridization analysis of *Hnf1b* showed that pseudoglandular cells strongly expressed *Hnf1b* mRNAs in the knockout liver, although *Hnf1b* expression was confined to periportal biliary epithelial cells in the wild-type liver (data, not shown). *Hnf6* and its protein expression were detectable in biliary epithelial cells and liver parenchymal cells in both the wild-type and knockout livers (data, not shown).

Relationships between expression of SOX9 and HNF1α or HNF4α in liver cell populations of wild-type and knockout livers were further examined using double immunohistochemical techniques. As a result, expression of SOX9 and HNF1α or HNF4α was found to be exclusive in the wild-type liver; biliary epithelial cells expressed SOX9 but not HNF1α or HNF4α, whereas hepatocytes expressed HNF1α and HNF4α but not SOX9 (Fig. 8A). In the knockout liver, their expression pattern was remarkably disordered in the

Table 4. Partial sequences of cDNAs used for making RNA probes in *in situ* hybridization analysis.

Symbol	GenBank	Sequence
Afp	NM_012493.2	a941~2020 (1080 b)
Alb	NM_134326.2	a1~716 (716 b)
Hnf1b	NM_009330.2	427~1118 (692 b)
Hnf6	NM_008262.3	1259~1729 (471 b)
Jag1	NM_013822.5	3191~3963 (773 b)
Sox9	NM_011448.4	2172~2938 (767 b)
Spp1	NM_001204203.1	45~538 (494 b)

[a]cDNAs of the rat. The numbers in parentheses denote sizes of each RNA probe.

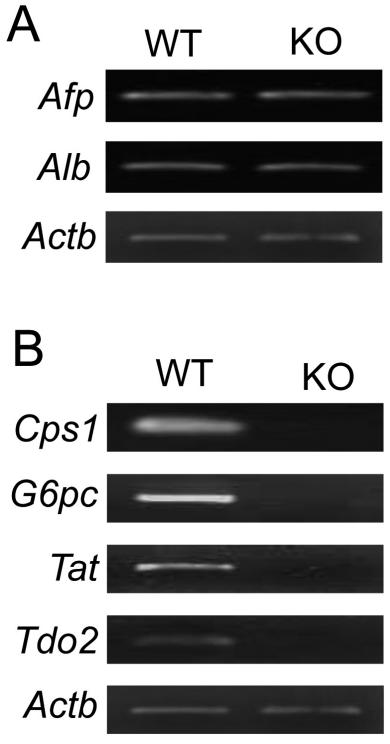

Fig. 2. RT-PCR analysis of gene expression of hepatocyte markers in E17.5 wild-type and knockout mouse livers. **A.** *Afp* and *Alb* expression. **B.** *Cps1, G6pc, Tat,* and *Tdo2* expression. While *Afp* and *Alb* expression is similar in wild-type and knockout livers **(A)**, expression of *Cps1, G6pc, Tat,* and *Tdo2* is remarkably reduced in the knockout liver **(B)**.

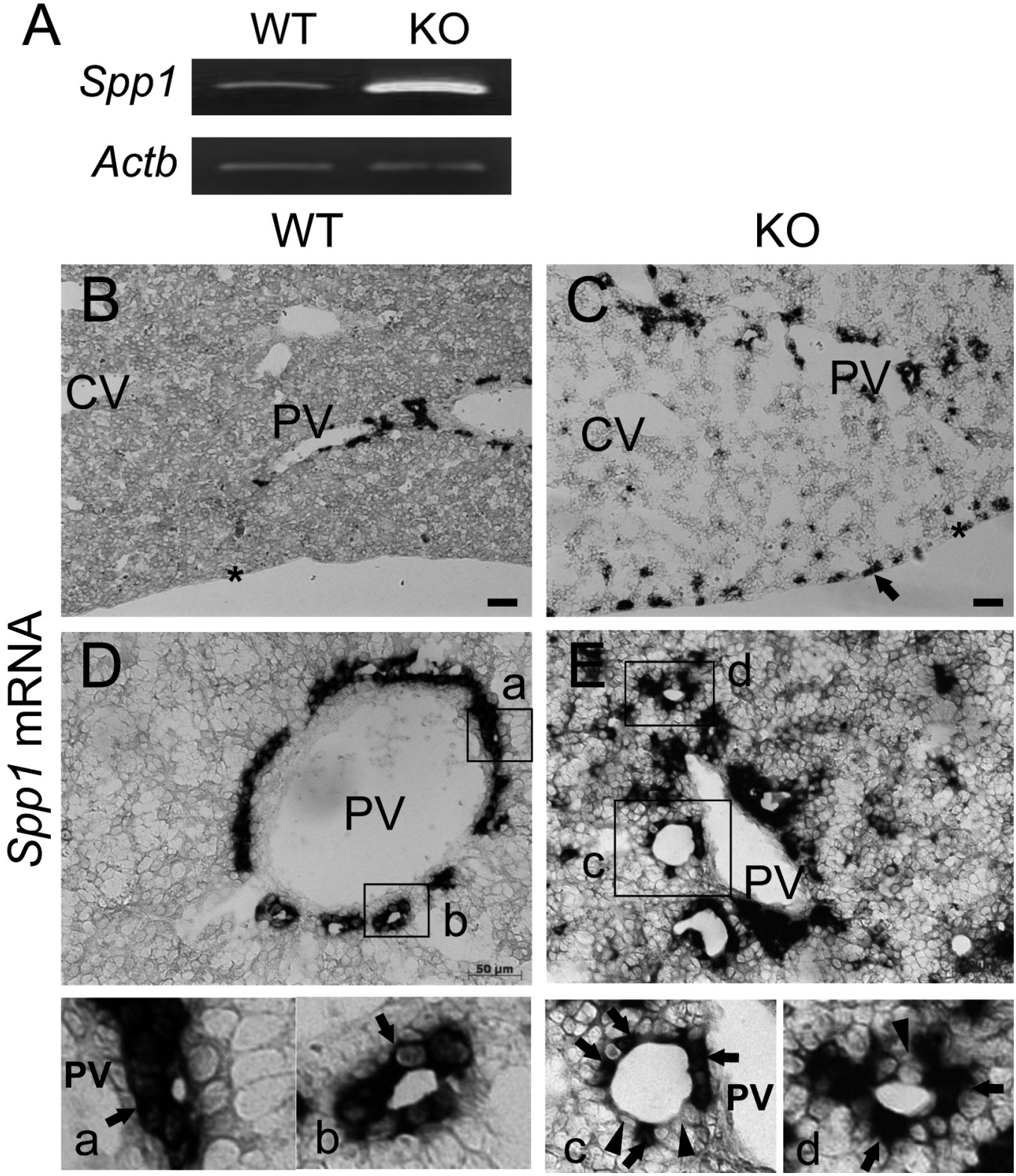

Fig. 3. Expression of *Spp1* in E17.5 wild-type and knockout livers. **A.** RT-PCR analysis of *Spp1* expression. *Spp1* mRNAs are abundantly expressed in the knockout liver. **B-E.** *In situ* hybridization analysis of *Spp1* expression in wild-type **(B, D)** and knockout **(C, E)** livers. **a, b.** Enlarged pictures of rectangles in **D**. **c, d.** Enlarged pictures of rectangles in **E**. *Spp1* expression in the wild-type liver is highly specific for periportal biliary epithelial cells (**B**, **D**; arrows in **a, b**). By contrast, *Spp1* expression in the knockout liver is heterogeneous and shows a mosaic pattern of positive cells and negative cells (arrows and arrowheads, respectively, in **c, d; C, E**). Spp1-positive cells are also detectable in the parenchymal regions, including the capsular regions (arrow in **C**). Asterisks indicate the hepatic capsule. CV, central vein; PV, portal vein. Bars: 50 *µ*m.

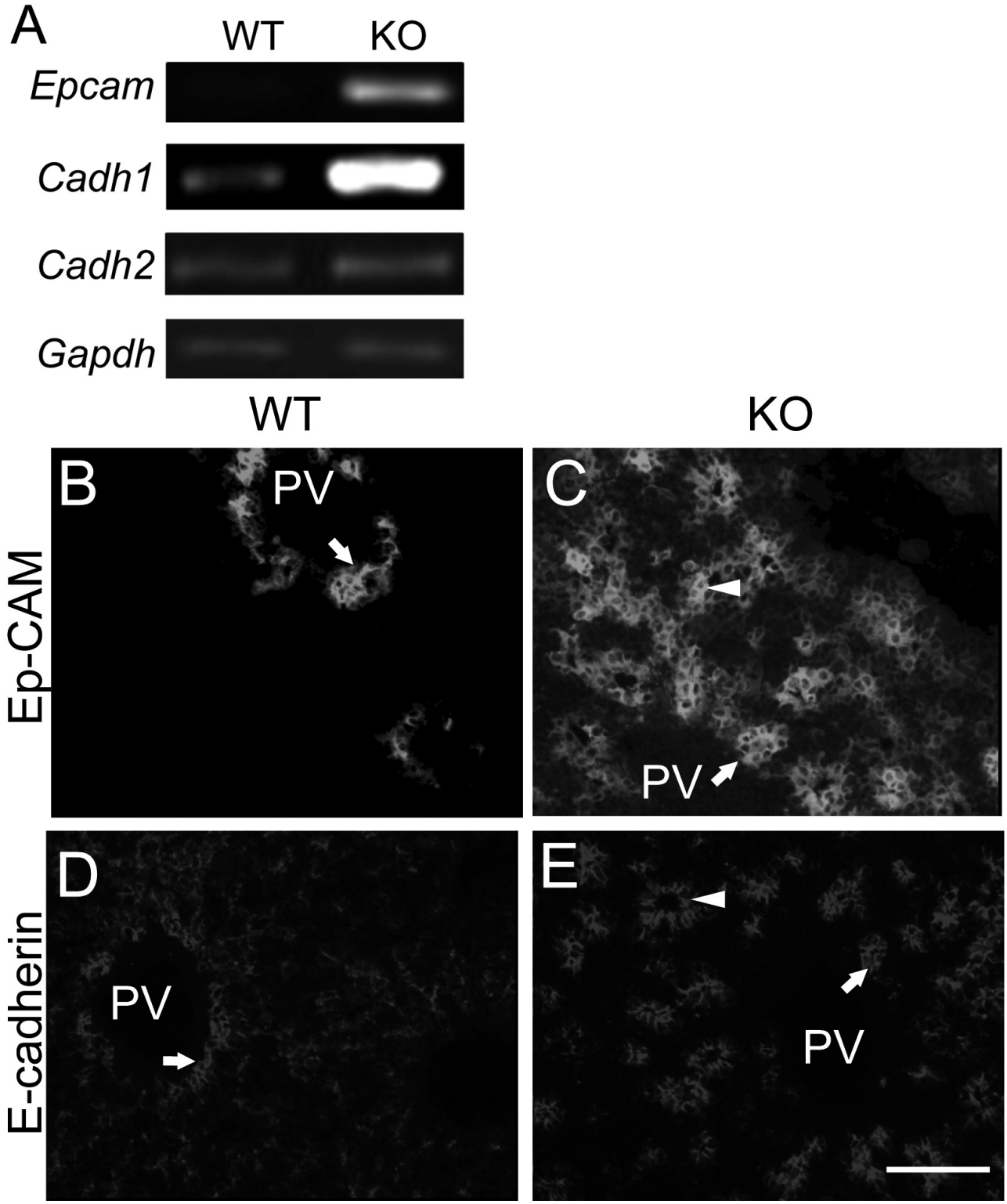

Fig. 4. Expression of Ep-CAM and E-cadherin in E17.5 wild-type and knockout livers. **A.** RT-PCR analysis of gene expression of cell adhesion molecules. Both *Epcam* and *Cadh1* (E-cadherin) mRNAs are abundantly expressed in the knockout livers. **B, C.** Ep-CAM immunohistochemistry. **D, E.** E-cadherin immunohistochemistry. Ep-CAM is expressed only in biliary epithelial cells of the wild-type liver (arrow) **(B)**. E-cadherin expression is weak or moderate in the liver parenchyma of the wild-type liver, while that in periportal biliary structures is strong (arrow) **(D)**. By contrast, expression of Ep-CAM and E-cadherin in the knockout liver is remarkably upregulated **(C, E)**, and most pseudoglandular cells, including periportal ones (arrows), are strongly positive. Arrowheads indicate pseudoglandular cells in the parenchyma regions. PV, portal vein. Bar: 50 μm.

parenchyma; HNF1α- and SOX9-positive cells, or SOX9-positive and HNF1α-negative cells, neither of which was observed in the wild-type liver parenchyma, were detectable in addition to HNF1α-positive but SOX9-negative cells (Fig. 8B). Similar data for SOX9 and HNF4α expression were obtained (data, not shown). Portal biliary structures were immature for expression of these transcription factors in the knockout liver, compared to those of the wild-type liver; the first layer of the ductal plates still contained SOX9- and HNF1α/HNF4α-positive cells, and the second layer consisted of cells having biliary gene expression in the knockout liver (Fig. 9A-C).

Phenotypes of nonparenchymal cells

To determine how the phenotypes of nonparenchymal cells were changed in the *Cebpa*-knockout liver, their histology and gene expression were examined. Histologically, many hematopoietic cells were present among the pseudoglandular structures in the E17.5 knockout liver. PECAM-1 expression, which is normally found in capillary endothelial cells but not in mature sinusoidal endothelial cells, was upregulated in the knockout liver (Fig. 10A, B). Desmin and vimentin-positive stellate cells also increased in perisinusoidal regions and around portal veins (Fig. 10C-F). Portal connective tissue was often thickened in the knockout liver (Figs. 10D, 11D). *Jag1* expression was also strongly detectable in the thickened portal mesenchyme and endothelial cells, although that in the capsular regions was negative (Fig. 11A-F). Comparatively heavy collagen deposition was seen in portal areas and pericapsular regions of the knockout liver (Fig. 12A-D). RT-PCR analysis of gene expression of nonparenchymal cell markers demonstrated that expression of *Pecam1, Des, Foxf1a* and *Jag1* was upregulated in the knockout liver (Figs. 10G, 11G).

Discussion

C/EBPα expression is required for both hepatocyte maturation and biliary morphogenesis

We have already shown that inactivation of the C/EBPα gene in mice induces pseudoglandular structures in the liver parenchyma, which highly express *Hnf6, Hnf1b, Jag1* and *Notch2*, but only those in periportal areas have a basal lamina and express bile duct-specific lectin-binding sites, suggesting that periportal microenvironments are indispensable for biliary differentiation in addition to the suppression of the C/EBPα expression in hepatoblasts (Yamasaki et al., 2006). The present study further demonstrated that inactivation of the C/EBPα gene caused not only prominent downregulation of liver-specific genes such as *Cps1, Tdo2, G6pc* and *Tat*, but also upregulation of genes for other biliary markers and biliary transcription factors, including *Spp1, Epcam,* and *Sox9* in addition to *Hnf6* and *Hnf1b*. These data suggest that C/EBPα is involved in switching of the differentiation of hepatoblasts into hepatocytes and biliary epithelial cells. C/EBPα can bind to upstream regulatory sequences of *Cps1, Tdo2, G6pc* and *Tat* genes and promote their transcription (Kimura et al., 1998; Nerlov, 2010; Tsukada et al., 2011). However, because the levels of gene expression for other liver-enriched transcription factors such as *Foxa2-3, Hnf1a* and *Hnf4a* did not differ between the wild-type and knockout livers, their transcription may be independent of the C/EBPα action at the developmental stage examined. This result is consistent with the Matrix RNAi data showing that the action of C/EBPα may be downstream from those of other liver-enriched transcription factors in an inter-transcription factor regulatory network in human hepatoma cells (Tomaru et al., 2009). In postnatal ablation of the *Cebpa* gene or its knockdown using siRNA in hepatocytes, expression of *Cebpb* and *Cebpd* is upregulated, but that of *Hnf4a* is not affected (Yang et

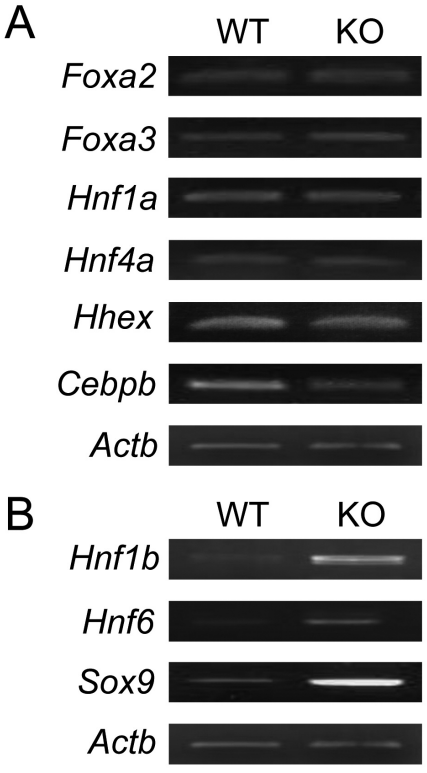

Fig. 5. RT-PCR analysis of gene expression of liver-enriched and biliary transcription factors in E17.5 wild-type and knockout mouse livers. **A.** Expression of mRNAs for liver-enriched transcription factors. **B.** Expression of mRNAs for transcription factors controlling biliary differentiation. While expression of liver-enriched transcription factors, except for that of *Cebpb*, does not differ between the wild-type and knockout livers, that of *Hnf1b, Hnf6* and *Sox9* mRNAs is upregulated in knockout livers. *Cebpb* expression is downregulated in the knockout liver.

al., 2005; Safdar et al., 2012). Although the results obtained in the current study demonstrated that *Cebpb* expression was downregulated in the fetal knockout liver, this finding is discrepant with the data obtained in the conditional knockout or siRNA studies. Transcriptional control of genes for other C/EBP members by C/EBPα may depend on the developmental stage or maturation state of the hepatocytes.

Because C/EBPα can functionally interact with other transcription factors to elicit transcriptional synergy (Yoshida et al., 2006; Benet et al., 2010), this mechanism may not work in the knockout liver, which can also result in impaired hepatocyte maturation. It is possible that the upregulated biliary transcription factors such as SOX9 and HNF1ß suppress transcription of hepatocyte-specific genes.

Our immunohistochemical and *in situ* hybridization studies demonstrated for the first time that the expression of biliary transcription factors SOX9 and *Hnf1b*, and of liver-enriched transcription factors HNF1α and HNF4α, was heterogeneous in the knockout liver, whereas the distribution of both types of transcription factors was mutually exclusive in the wild-type liver; the former and latter were expressed in biliary epithelial cells and hepatocytes, respectively. Some biliary epithelial cells or biliary epithelial cell-like cells, which expressed SOX9 and *Spp1* protein but not HNF1α and HNF4α, appeared in the knockout pseudoglandular structures in nonperiportal areas, especially in pericapsular and pericentral areas, indicating that the deficiency of C/EBPα directly induced biliary cell differentiation in hepatoblasts without induction from periportal mesenchymal cells. It is unknown at present why mosaic or stochastic expression of biliary markers and transcription factors occurs in the knockout liver. Perhaps these patterns are related to the intrinsic nature of hepatoblasts, which may autonomously generate both cell types without C/EBPα, or to cellular interactions with nonparenchymal cells. It is possible that the presence of C/EBPα may be a prerequisite for hepatocyte maturation, or may stabilize the phenotype of hepatocytes. It is noteworthy that *Sox9* and its protein expression were highly upregulated in the knockout liver, suggesting that gene expression of this transcription factor may be downstream of the C/EBPα action or may be exclusive to that of C/EBPα.

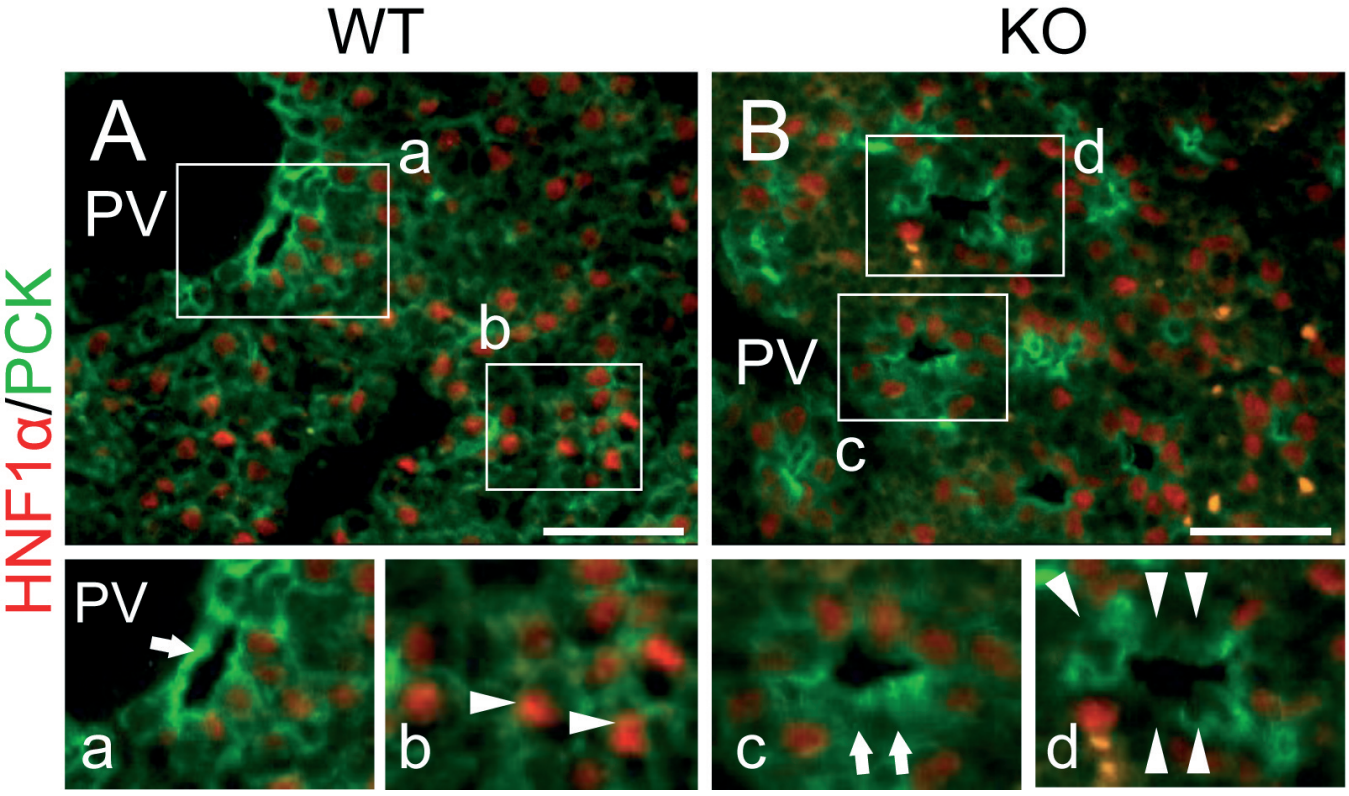

Fig. 6. Expression of HNF1α in E17.5 wild-type **(A)** and knockout **(B)** livers. **A, B.** Double immunofluorescence of HNF1α and cytokeratins with polyclonal anti-calf keratins. **a, b.** Enlarged pictures of rectangles in **A**. **c, d.** Enlarged pictures of rectangles in **B**. Expression of HNF1α occurs in all hepatocytes of the liver parenchyma of the wild-type **(A).** Asymmetric expression of HNF1α is detectable in periportal bile duct structures (arrows in **a**); negative cells on the portal side and positive cells on the parenchymal side. Arrowheads in **b** indicate HNF1α -positive cells in the parenchyma Expression of HNF1α in the knockout liver is heterogeneous, and exhibits a mosaic pattern of positive cells and negative cells in pseudoglandular structures **(B, c, d)**. Arrows and arrowheads indicate HNF1α –negative cells in pseudoglandular structures of periportal regions and parenchymal regions, respectively **(c, d)**. PV, portal vein. Bars: 50 μm.

Inactivation of the *Sox9* gene causes persistent expression of C/EBPα in periportal biliary epithelial cells (Antoniou et al., 2009). *Sox9* may be a target of Notch signaling (Delous et al., 2012; Martini et al., 2012). Thus, the elevated expression of *Jag1* in pseudoglandular structures of the knockout liver can cause upregulation of *Sox9* expression. On the contrary, SOX9 function may be required to maintain Notch signaling in the biliary cells. Because SOX9 was expressed with *Spp1* protein in biliary progenitors at early stages of liver development (E13.5-14.5; data not shown), it may play an important role in early biliary differentiation. SOX9 can directly control the gene expression of *Spp1* in early liver development (Pritchett

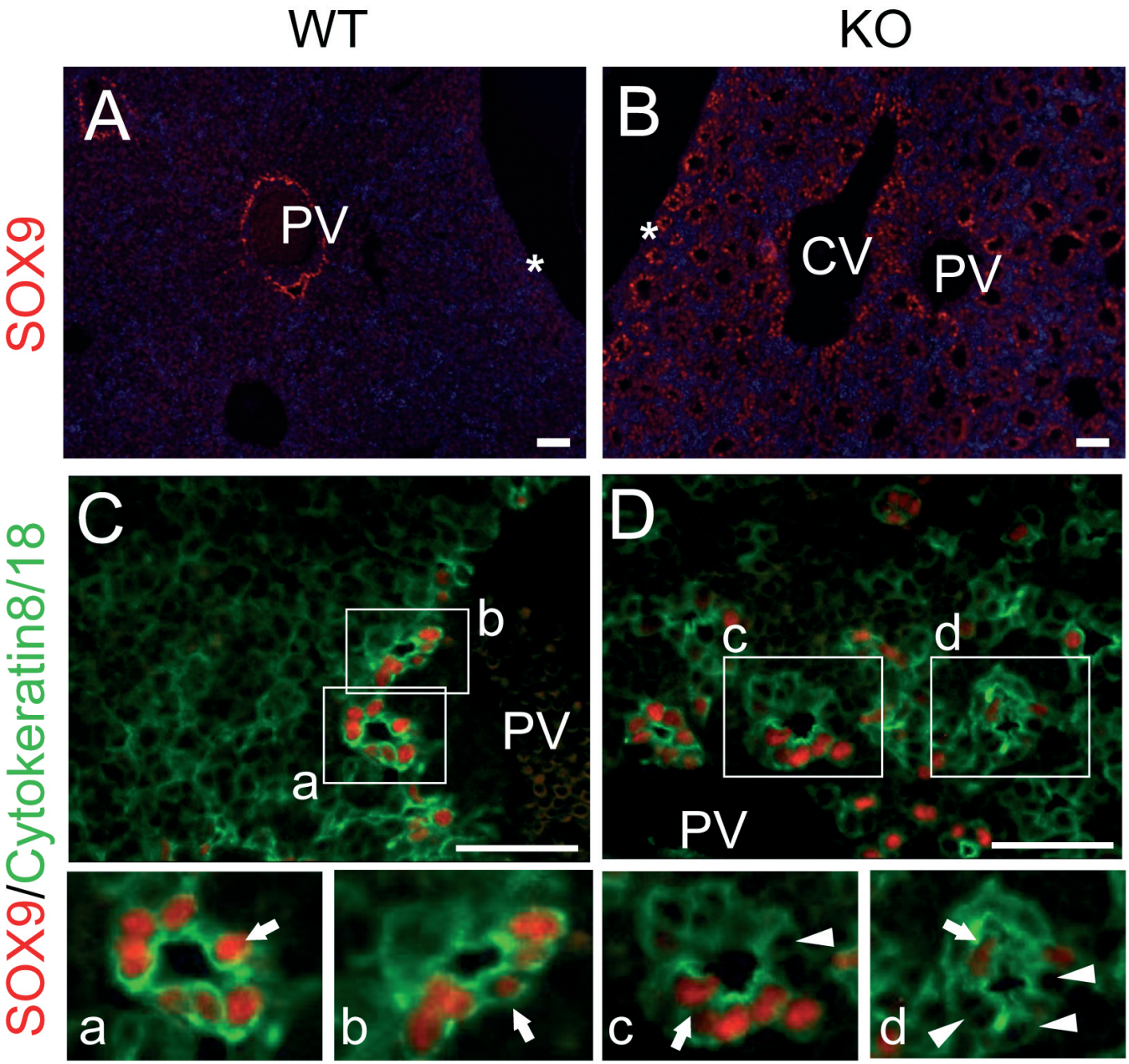

Fig. 7. Expression of SOX9 protein in E17.5 wild-type (**A, C**) and knockout (**B, D**) livers. **A, B.** SOX9 immunohistochemistry. **C, D.** Double immunofluorescence of SOX9 and cytokeratin 8/18 expression. **a, b.** Enlarged pictures of rectangles in **C**. **c, d.** Enlarged pictures of rectangles in **D**. SOX9 is expressed only in biliary epithelial cells around portal veins of the wild-type liver (**A, C**; arrows in **a, b**). By contrast, SOX9 expression is detectable in not only periportal biliary epithelial cells but also in pseudoglandular cells around central veins and under the hepatic capsule (asterisk) of the knockout liver (**B, D**). Arrows and arrowheads indicate SOX9-positive and negative cells in pseudoglandular structures, respectively (**c, d**). CV, central vein; PV, portal vein. Bars: 50 μm.

et al., 2012).

Although forced knockout of the *Cebpa* gene promoted biliary gene expression as discussed, periportal biliary structures may be immature as shown in the present study. The ductal plate structures had mosaic expression of *Spp1, Sox9, Hnf1b*, HNF1α and HNF4α, and their ductal morphogenesis was not completed in the knockout liver. It is unknown why, even in portal areas where the bile duct-inductive mesenchyme also resided in the knockout liver, normal bile duct morphogenesis did not happen. The mosaic expression of biliary markers in the ductal plates may be related to this abnormal biliary morphogenesis. All pseudoglandular cells of the knockout liver parenchyma abundantly expressed Ep-CAM and E-cadherin like periportal biliary cells. This abnormal expression of the adhesion molecules may be involved in the delayed ductal morphogenesis. Thickening of connective tissues might be related to the abnormality. In any case, hepatocyte maturation through C/EBPα expression that is not normally detectable in biliary epithelial cells may be required for normal bile differentiation and morphogenesis. In other words, novel cell-cell interactions or tissue interactions may occur between hepatocytes and biliary epithelial cells.

Biliary gene expression in Cebpa-deficient pseudoglandular cells of pericentral and pericapsular regions

Although pseudoglandular cells were abundantly developed in the whole liver parenchyma of the knockout fetus, those near the hepatic capsule preferentially expressed biliary markers such as SOX9, *Spp1* and *Hnf1b* at slightly lower levels than those in periportal areas. Some pericentral pseudoglandular cells also highly expressed these biliary markers. However, these pseudoglandular cells did not have a ductal morphology. Because pericapsular regions have abundant extracellular matrices and pericentral regions also have significantly more extracellular matrices than other liver parenchymal regions (Shiojiri and Sugiyama, 2004), their extracellular matrices may induce biliary gene expression when the C/EBPα expression is suppressed. However, capsular cells and mesenchymal cells of hepatic veins did not express *Jag1*, in contrast to its strong expression in portal mesenchymal and

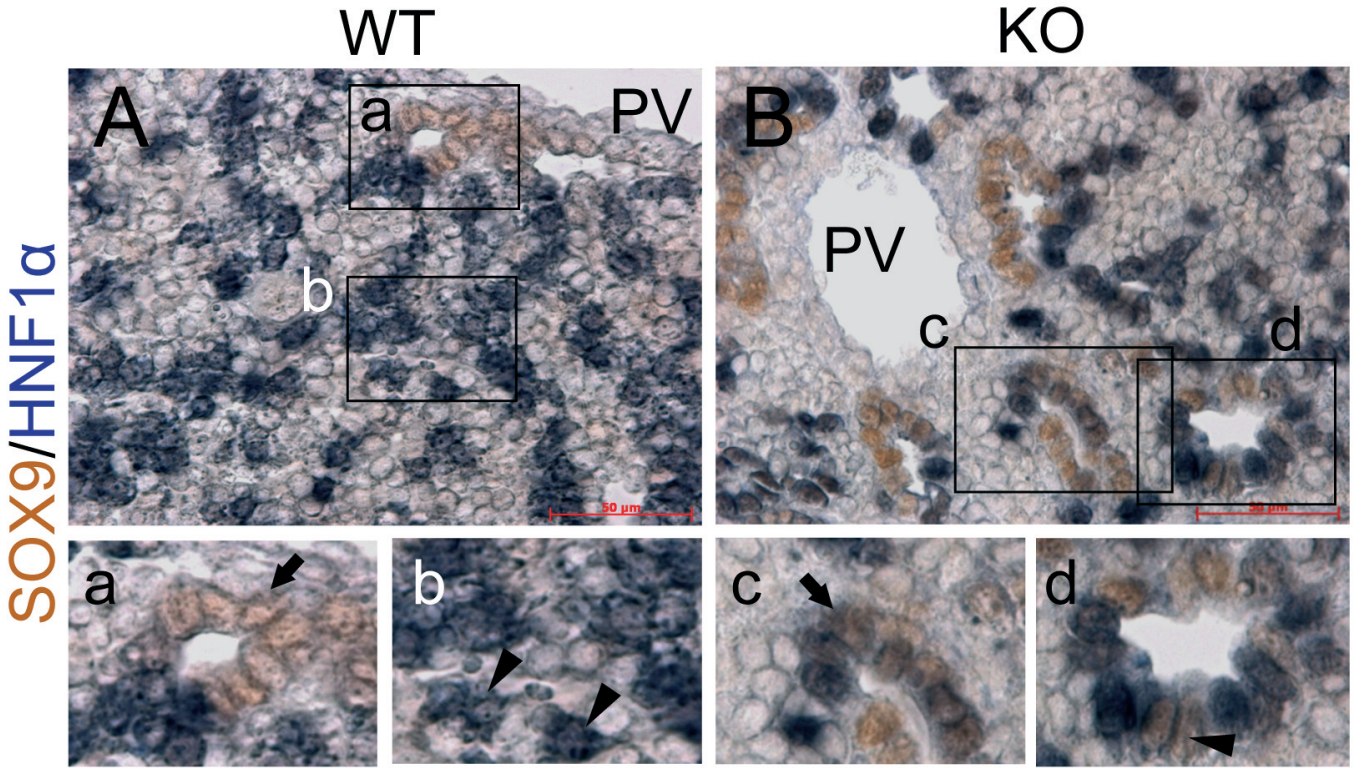

Fig. 8. Double immunohistochemical analysis of SOX9 and HNF1α in E17.5 wild-type **(A)** and knockout **(B)** livers. **A, B.** Double immunostaining of SOX9 (brown) and HNF1α (purple). **a, b.** Enlarged pictures of rectangles in A. **c, d.** Enlarged pictures of rectangles in **B**. Periportal biliary epithelial cells express SOX9, but not HNF1α in the wild-type liver (**A**; arrows in **a**). Hepatocytes in the parenchyma are positive for HNF1α, but negative for SOX9 (**A**; arrowheads in **b**). By contrast, in the knockout liver, some epithelial cells around portal veins are HNF1α- and SOX9-positive (**B**; arrow in **c**). SOX9 expression is also detectable in the liver parenchyma **(B)**. Arrowhead in **d** indicates HNF1α- and SOX9-positive cells in the parenchyma. PV, portal vein. Bars: 50 μm.

endothelial cells in the knockout liver. *Jag1* expression was also absent or very weak in pseudoglandular cells of pericapsular and pericentral regions, whereas periportal biliary epithelial cells highly expressed *Jag1* in both the wild-type and knockout livers. *Jag1* expression in both cells of portal veins and biliary epithelial cells may be important for normal biliary differentiation and morphogenesis.

Hepatocyte maturation affects gene expression and histogenesis of nonparenchymal cells

Impaired hepatocyte maturation through *Cebpa* inactivation also changed the phenotypes of other

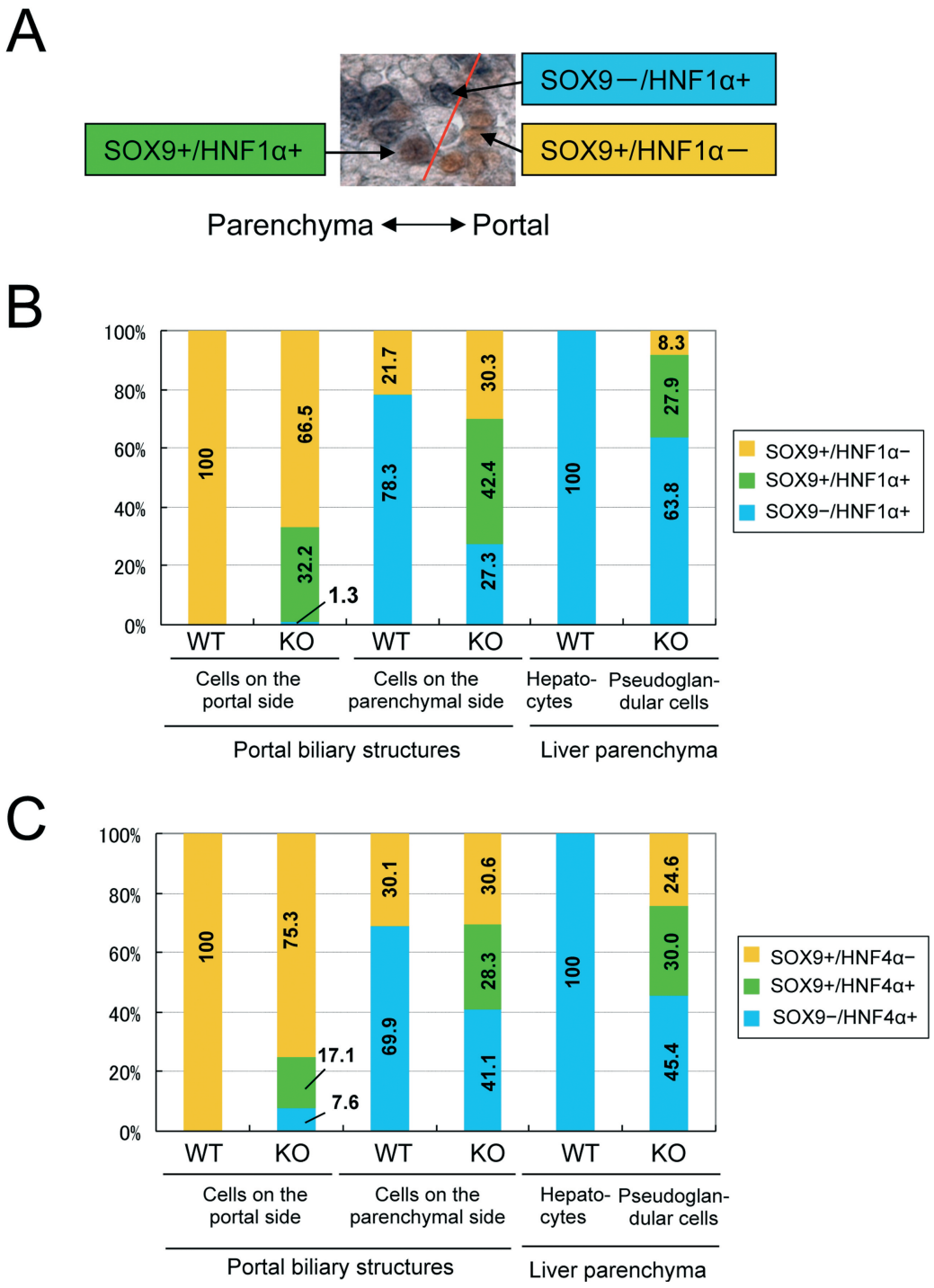

Fig. 9. Double immunohistochemical analysis of expression of SOX9 and HNF1α or HNF4α in E17.5 wild-type and knockout livers. **A.** Double immunostaining of SOX9 and HNF1α in an E17.5 knockout liver. Biliary epithelial cells adjacent to a portal vein express SOX9, but not HNF1α. Cells on the side of the liver parenchyma of the biliary structure express both SOX9 and HNF1α, or express HNF1α, but not SOX9. **B.** Expression of HNF1α and SOX9. **C.** Expression of HNF4α and SOX9. Although biliary differentiation (SOX9-positive, and HNF1α- or HNF4α-negative cells) occurs in some pseudoglandular cells of the knockout liver parenchyma, its periportal biliary differentiation is immature, especially in epithelial cells on the portal side, of biliary structures (ductal plates), in which immature biliary cells are still detectable.

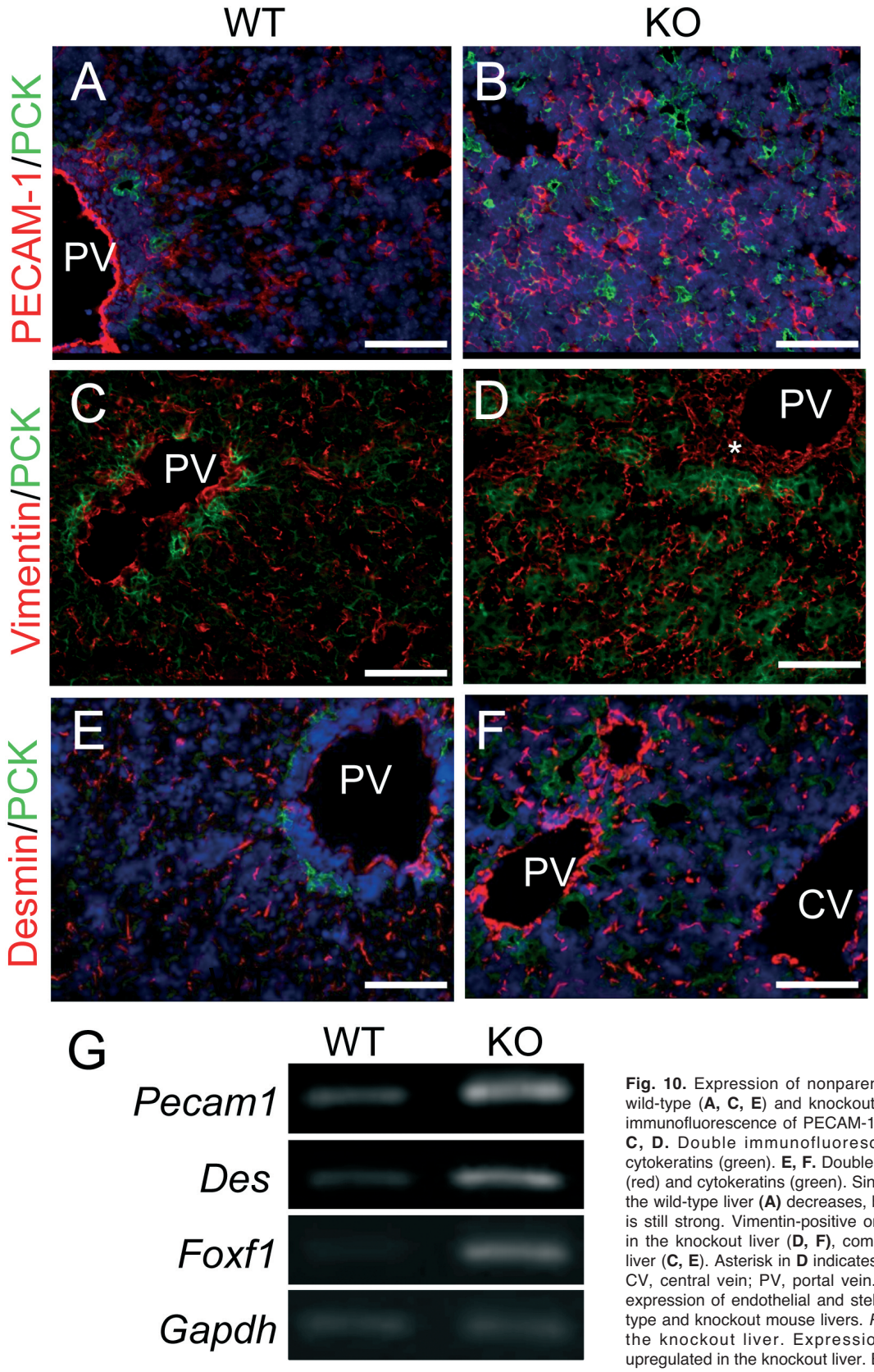

Fig. 10. Expression of nonparenchymal cell markers in E17.5 wild-type (**A, C, E**) and knockout (**B, D, F**) livers. **A, B.** Double immunofluorescence of PECAM-1 (red) and cytokeratins (green). **C, D.** Double immunofluorescence of vimentin (red) and cytokeratins (green). **E, F.** Double immunofluorescence of desmin (red) and cytokeratins (green). Sinusoidal PECAM-1 expression in the wild-type liver **(A)** decreases, but that in the knockout liver **(B)** is still strong. Vimentin-positive or desmin-positive cells increase in the knockout liver (**D, F**), compared to those in the wild-type liver (**C, E**). Asterisk in **D** indicates thickened portal mesenchyme. CV, central vein; PV, portal vein. **G.** RT-PCR analyses of gene expression of endothelial and stellate cell markers in E17.5 wild-type and knockout mouse livers. *Pecam1* expression increases in the knockout liver. Expression of *Des* and *Foxf1* is also upregulated in the knockout liver. Bars: 100 μm.

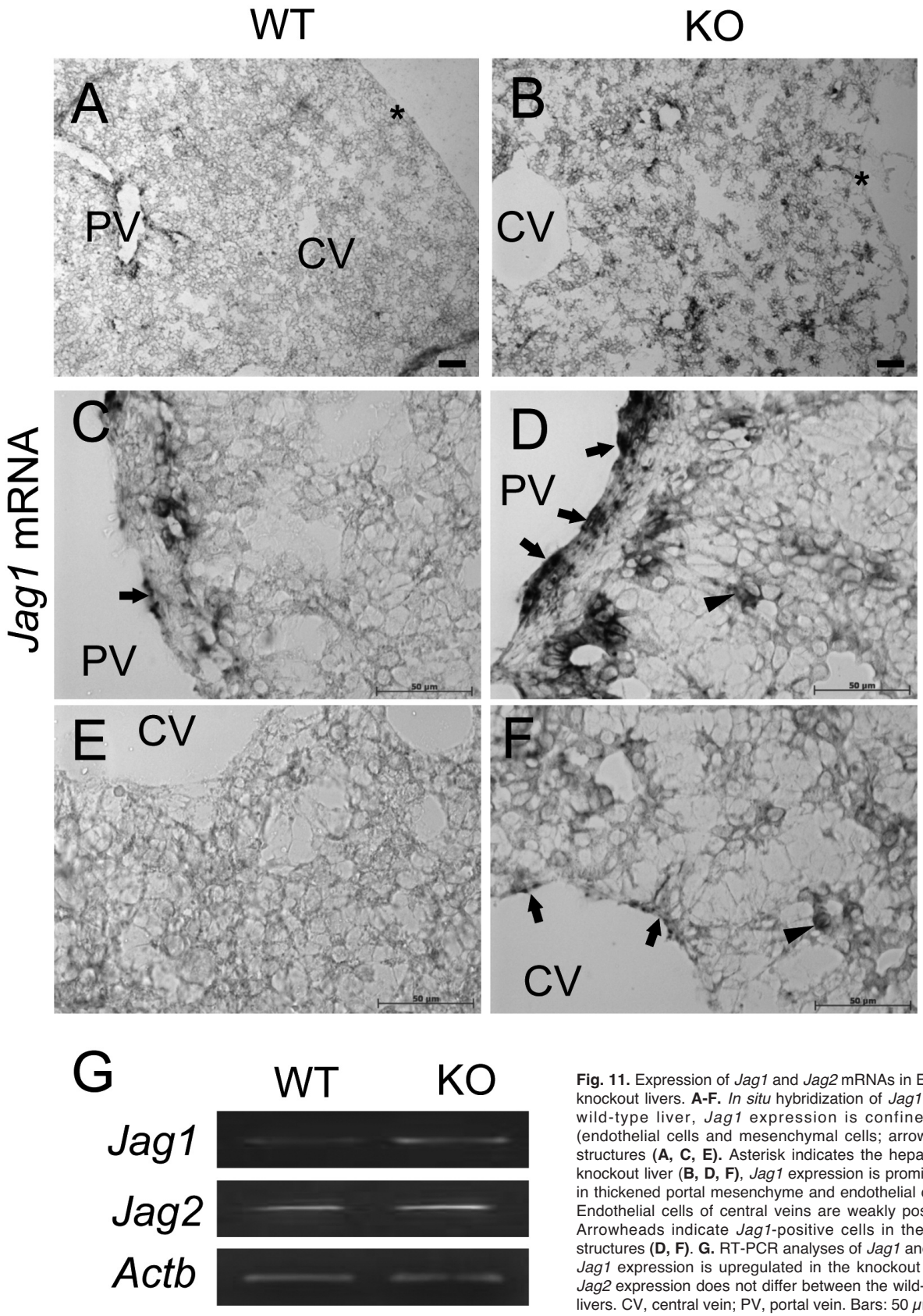

Fig. 11. Expression of *Jag1* and *Jag2* mRNAs in E17.5 wild-type and knockout livers. **A-F.** *In situ* hybridization of *Jag1* expression. In the wild-type liver, *Jag1* expression is confined to portal cells (endothelial cells and mesenchymal cells; arrow in **C**) and biliary structures (**A, C, E).** Asterisk indicates the hepatic capsule. In the knockout liver (**B, D, F)**, *Jag1* expression is prominently upregulated in thickened portal mesenchyme and endothelial cells (arrows in **D**). Endothelial cells of central veins are weakly positive for *Jag1* (**F**). Arrowheads indicate *Jag1*-positive cells in the pseudoglandular structures **(D, F)**. **G.** RT-PCR analyses of *Jag1* and *Jag2* expression. *Jag1* expression is upregulated in the knockout liver. The level of *Jag2* expression does not differ between the wild-type and knockout livers. CV, central vein; PV, portal vein. Bars: 50 μm.

nonparenchymal cells in addition to the abnormal biliary differentiation and morphogenesis, with thickening of the portal mesenchyme, increased expression of stellate cell marker genes (*Des* and *Foxf1*), increased deposition of collagens, and the immature state of sinusoidal endothelial cells (PECAM-1 expression). These data indicated that hepatocyte maturation through C/EBPα expression might suppress abnormal fibrosis and stimulate mature sinusoid development, and that C/EBPα expression in hepatocytes was indispensable for normal nonparenchymal tissue development. Our data agreed well with the conclusion that nonparenchymal cells intimately interact with hepatocytes to construct functional liver lobules, which was derived from *in vitro* culture studies (Matsumoto et al., 2001; Deleve et al., 2008; March et al., 2009; Takabe et al., 2012).

Many hematopoietic cells were still observed in the knockout livers at E17.5 and P0, compared with the wild-type livers. This phenomenon may be related to impaired hepatocyte maturation through *Cebpa* gene inactivation. It has been shown that the signals exerted by oncostatin M and glucocorticoid induce hepatic differentiation, which in turn terminate embryonic hematopoiesis and promote relocation of hematopoietic cells (Kinoshita et al., 1999).

Conclusions

Inactivation of the *Cebpa* gene induces heterogeneous and improper expression of other liver-

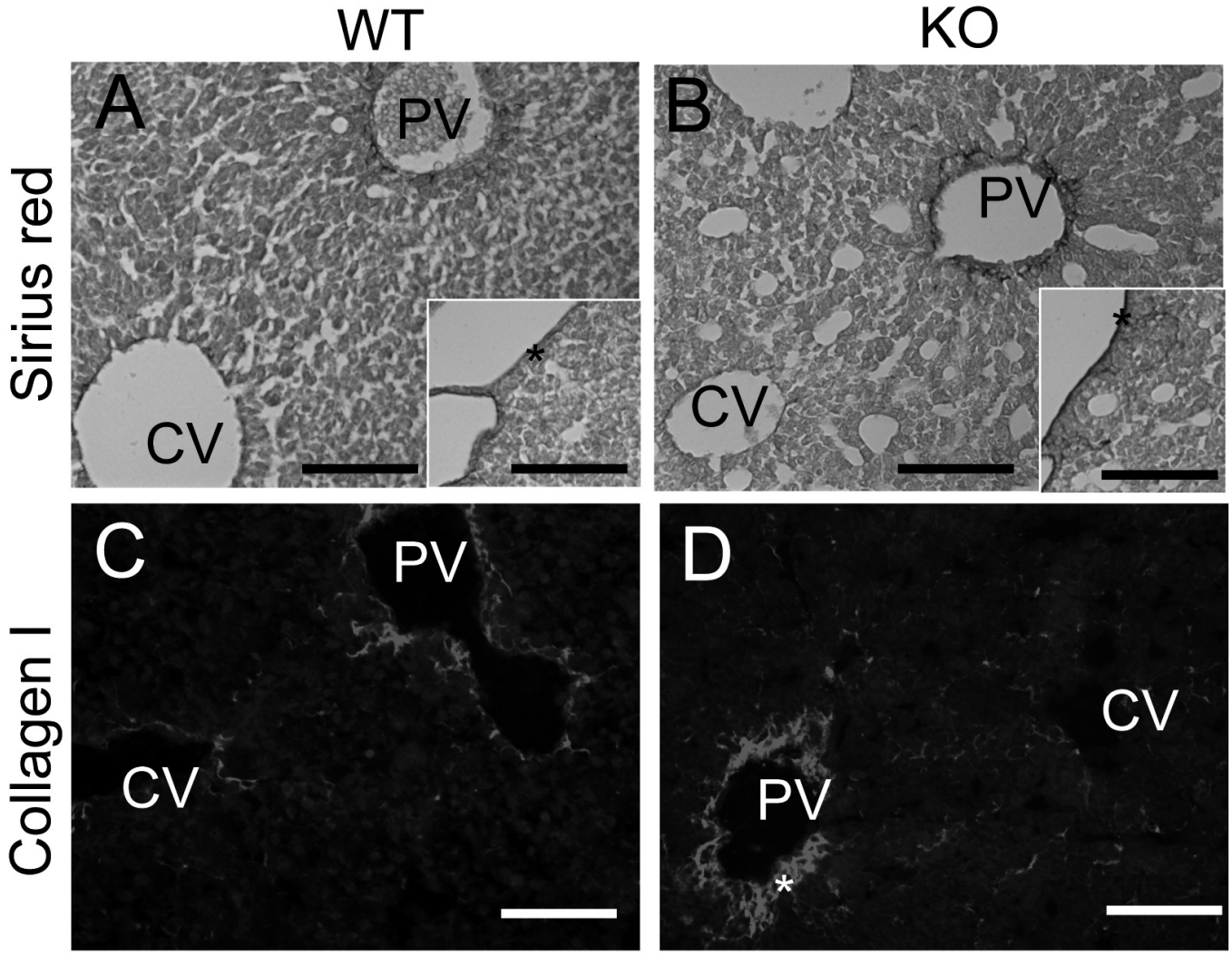

Fig. 12. Deposition of extracellular matrices in E17.5 wild-type (**A, C**) and knockout (**B, D**) livers. **A, B.** Sirius red staining. **C, D.** Type I collagen immunofluorescence. Sirius red-positive collagens are more heavily deposited in portal areas and capsular regions of the knockout liver than in the wild-type liver (**A, B**). Asterisk in **A, B** indicates the hepatic capsule. The deposition of type I collagen is heavier in portal regions of the knockout liver than that in the wild-type liver (**C, D**). Asterisk in **D** indicates thickened portal mesenchyme. CV, central vein; PV, portal vein. Bars: 100 μm.

enriched transcription factors such as HNF1α and HNF4α, biliary transcription factors such as SOX9 and *Hnf1b*, and biliary markers, including *Spp1* protein and Ep-CAM, in the liver parenchyma. C/EBPα expression may stabilize the differentiation state of hepatocytes. Nonparenchymal cell development, including bile and vascular systems, requires normal maturation of the liver parenchyma through C/EBPα expression in hepatocytes.

Acknowledgments. We thank Professor Emeritus Takeo Mizuno of the University of Tokyo and Prof. Nelson Fausto of the University of Washington for their interest in our study and encouragement, and Mr. Kim Barrymore for his help in preparing our manuscript. This work was supported in part by MEXT/JSPS KAKENHI Grant Number 22570063. This work was also supported in part by a Sasakawa Scientific Research Grant from the Japan Science Society to Y. Akai.

References

Antoniou A., Raynaud P., Cordi S., Zong Y., Tronche F., Stanger B.Z., Jacquemin P., Pierreux C.E., Clotman F. and Lemaigre F.P. (2009). Intrahepatic bile ducts develop according to a new mode of tubulogenesis regulated by the transcription factor SOX9. Gastroenterology 136, 2325-2333.

Benet M., Lahoz A., Guzmán C., Castell J.V. and Jover R. (2010). CCAAT/enhancer-binding protein α (C/EBPα) and hepatocyte nuclear factor 4α (HNF4α) synergistically cooperate with constitutive androstane receptor to transactivate the human cytochrome P450 2B6 (CYP2B6) gene: application to the development of a metabolically competent human hepatic cell model. J. Biol. Chem. 285, 28457-28471.

Carpentier R., Suñer R.E., van Hul N., Kopp J.L., Beaudry J.B., Cordi S., Antoniou A., Raynaud P., Lepreux S., Jacquemin P., Leclercq I.A., Sander M. and Lemaigre F.P. (2011). Embryonic ductal plate cells give rise to cholangiocytes, periportal hepatocytes, and adult liver progenitor cells. Gastroenterology 141, 1432-1438.

Clotman F., Jacquemin P., Plumb-Rudewiez N., Pierreux C.E., Van der Smissen P., Dietz H.C., Courtoy P.J., Rousseau G.G. and Lemaigre F.P. (2005). Control of liver cell fate decision by a gradient of TGFb signaling modulated by Onecut transcription factors. Genes Dev. 19, 1849-1854.

Clotman F., Lannoy V.J., Reber M., Cereghini S., Cassiman D., Jacquemin P., Roskams T., Rousseau, G.G. and Lemaigre F.P. (2002). The onecut transcription factor HNF6 is required for normal development of the biliary tract. Development 129, 1819-1828.

Coffinier C., Gresh L., Fiette L., Tronche F., Schutz G., Babinet C., Pontoglio M., Yaniv M. and Barra J. (2002). Bile system morphogenesis defects and liver dysfunction upon targeted deletion of HNF1ß. Development 129, 1829-1838.

Deleve L.D., Wang X. and Guo Y. (2008). Sinusoidal endothelial cells prevent rat stellate cell activation and promote reversion to quiescence. Hepatology 48, 920-930.

Delous M., Yin C., Shin D., Ninov N., Debrito Carten J., Pan L., Ma T.P., Farber S.A., Moens C.B. and Stainier D.Y. (2012). Sox9b is a key regulator of pancreaticobiliary ductal system development. PLoS Genet. 8, e1002754.

Flodby P., Barlow C., Kylefjord H., Åhrlund-Richter L. and Xanthopoulos K.G. (1996). Increased hepatic cell proliferation and lung abnormalities in mice deficient in CCAAT/enhancer binding protein ·. J. Biol. Chem. 271, 24753-24760.

Hofmann J.J., Zovein A.C., Koh H., Radtke F., Weinmaster G. and Iruela-Arispe M.L. (2010). Jagged1 in the portal vein mesenchyme regulates intrahepatic bile duct development: insights into Alagille syndrome. Development 137, 4061-4072.

Ishii Y., Fukuda K., Saiga H., Matsushita S. and Yasugi S. (1997). Early specification of intestinal epithelium in the chicken embryo: a study on the localization and regulation of CdxA expression. Dev. Growth Differ. 39, 643-653.

Johnson G.D. and de C. Nogueira Araujo G.M. (1981). A simple method of reducing the fading of immunofluorescence during microscopy. J. Immunol. Methods 43, 349-350.

Junqueira L.C., Bignolas G. and Brentani R.R. (1979). Picrosirius staining plus polarization microscopy, a specific method for collagen detection in tissue sections. Histochem. J. 11, 447-455.

Kimura T., Christoffels V.M., Chowdhury S., Iwase K., Matsuzaki H., Mori M., Lamers W.H., Darlington G.J. and Takiguchi M. (1998). Hypoglycemia-associated hyperammonemia caused by impaired expression of ornithine cycle enzyme gene in C/EBPα knockout mice. J. Biol. Chem. 273, 27505-27510.

Kinoshita T., Sekiguchi T., Xu M.J., Ito Y., Kamiya A., Tsuji K., Nakahata T. and Miyajima A. (1999). Hepatic differentiation induced by oncostatin M attenuates fetal liver hematopoiesis. Proc. Natl. Acad. Sci. USA 96, 7265-7270.

Landschulz W.H., Johnson P.F. and McKnight S.L. (1989). The DNA binding domain of the rat liver nuclear protein C/EBP is bipartite. Science 243, 1681-1688.

March S., Hui E.E., Underhill G.H., Khetani S. and Bhatia S.N. (2009). Microenvironmental regulation of the sinusoidal endothelial cell phenotype in vitro. Hepatology 50, 920-928.

Martini S., Bernoth K., Main H., Dario Camargo Ortega G., Lendahl U., Just U. and Schwanbeck R. (2012). A critical role for Sox9 in notch-induced astrogliogenesis and stem cell maintenance. Stem Cells 31,741-751.

Matsumoto K., Yoshitomi H., Rossant J. and Zaret K.S. (2001). Liver organogenesis promoted by endothelial cells prior to vascular function. Science 294, 559-563.

McCright B., Lozier J. and Gridley T. (2002). A mouse model of Alagille syndrome: Notch2 as a genetic modifier of Jag1 haploinsufficiency. Development 129, 1075-1082.

Nerlov C. (2010). Transcriptional and translational control of C/EBPs: the case for "deep" genetics to understand physiological function. Bioessays 32, 680-686.

Pritchett J., Harvey E., Athwal V., Berry A., Rowe C., Oakley F., Moles A., Mann D.A., Bobola N., Sharrocks A.D., Thomson B.J., Zaitoun A.M., Irving W.L., Guha I.N., Hanley N.A. and Hanley K.P. (2012). Osteopontin is a novel downstream target of SOX9 with diagnostic implications for progression of liver fibrosis in humans. Hepatology 56, 1108-1116.

Safdar H., Cheung K.L., Vos H.L., Gonzalez F.J., Reitsma P.H., Inoue Y. and van Vlijmen B.J. (2012). Modulation of mouse coagulation gene transcription following acute in vivo delivery of synthetic small interfering RNAs targeting HNF4α and C/EBPα. PLoS One 7, e38104.

Sargent T.D., Yang M. and Bonner J. (1981). Nucleotide sequence of cloned rat serum albumin messenger RNA. Proc. Natl. Acad. Sci. USA 78, 243-246.

Shiojiri N. (1994). Transient expression of bile duct-specific cytokeratin

by fetal mouse hepatocytes. Cell Tissue Res. 278, 117-123.

Shiojiri N. (1997). Development and differentiation of bile ducts in the mammalian liver. Microsc. Res. Tech. 39, 328-335.

Shiojiri N. and Sugiyama Y. (2004). Immunolocalization of extracellular matrix components and integrins during mouse liver development. Hepatology 40, 346-355.

Shiojiri N., Lemire J.M. and Fausto N. (1991). Cell lineages and oval cell progenitors in rat liver development. Cancer Res. 51, 2611-2620.

Si-Tayeb K., Lemaigre F.P. and Duncan S.A. (2010). Organogenesis and development of the liver. Dev. Cell 18, 175-189.

Takabe Y., Yagi S., Koike T. and Shiojiri N. (2012). Immunomagnetic exclusion of E-cadherin-positive hepatoblasts in fetal mouse liver cell cultures impairs morphogenesis and gene expression of sinusoidal endothelial cells. J. Anat. 221, 229-239.

Tanaka M., Okabe M., Suzuki K., Kamiya Y., Tsukahara Y., Saito S. and Miyajima A. (2009). Mouse hepatoblasts at distinct developmental stages are characterized by expression of Ep-CAM and DLK1: drastic change of Ep-CAM expression during liver development. Mech. Dev. 126, 665-676.

Tanimizu N. and Miyajima A. (2004). Notch signaling controls hepatoblast differentiation by altering the expression of liver-enriched transcription factors. J. Cell Sci. 117, 3165-3174.

Tomaru Y., Nakanishi M., Miura H., Kimura Y., Ohkawa H., Ohta Y., Hayashizaki Y. and Suzuki M. (2009). Identification of an inter-transcription factor regulatory network in human hepatoma cells by Matrix RNAi. Nucleic Acids Res. 37, 1049-1060.

Tomizawa M., Garfield S., Factor V. and Xanthopoulos K.G. (1998). Hepatocytes deficient in CCAAT/enhancer binding protein α (C/EBPα) exhibit both hepatocyte and biliary epithelial cell character. Biochem. Biophys. Res. Comm. 249, 1-5.

Tsukada J., Yoshida Y., Kominato Y. and Auron P.E. (2011). The CCAAT/enhancer (C/EBP) family of basic-leucine zipper (bZIP) transcription factors is a multifaceted highly-regulated system for gene regulation. Cytokine 54, 6-19.

Van Eyken P., Sciot R., Callea F., Van der Steen K., Moerman P. and Desmet V.J. (1988a). The development of the intrahepatic bile ducts in man: A keratin-immunohistochemical study. Hepatology 8, 1586-1595.

Van Eyken P., Sciot R. and Desmet V. (1988b). Intrahepatic bile duct development in the rat: A cytokeratin-immunohistochemical study. Lab. Invest. 59, 52-59.

Wang N.-D., Finegold M.J., Bradley A., Ou C.N., Abdelsayed S.V., Wilde M.D., Taylor L.R., Wilson D.R. and Darlington G.J. (1995). Impaired energy homeostasis in C/EBP a knockout mice. Science 269, 1108-1112.

Xanthopoulos K.G., Mirkovitch J., Decker T., Kuo C.F. and Darnell J.E., Jr. (1989). Cell-specific transcriptional control of the mouse DNA-binding protein mC/EBP. Proc. Natl. Acad. Sci. USA 86, 4117-4121.

Yamasaki H., Sada A., Iwata T., Niwa T., Tomizawa M., Xanthopoulos K.G., Koike T. and Shiojiri N. (2006). Suppression of C/EBP· expression in periportal hepatoblasts may stimulate biliary cell differentiation through increased Hnf6 and Hnf1b expression. Development 133, 4233-4243.

Yang J., Croniger C.M., Lekstrom-Himes J., Zhang P., Fenyus M., Tenen D.G., Darlington G.J. and Hanson R.W. (2005). Metabolic response of mice to a postnatal ablation of CCAAT/enhancer-binding protein alpha. J. Biol. Chem. 280, 38689-38699.

Yoshida Y., Hughes D.E., Rausa F.M. 3rd, Kim I.M., Tan Y., Darlington G.J. and Costa R.H. (2006). C/EBPa and HNF6 protein complex formation stimulates HNF6-dependent transcription by CBP coactivator recruitment in HepG2 cells. Hepatology 43, 276-286.

Accepted July 11, 2013